

**Picosecond Infrared Vibrational Photon Echoes in a Liquid and Glass Using a Free Electron Laser**

David Zimdars, A. Tokmakoff, S. Chen, S. R. Greenfield, and M. D. Fayer  
*Department of Chemistry, Stanford University, Stanford, California 94305*

T. I. Smith and H. A. Schwettman  
*Department of Physics, Stanford University, Stanford, California 94305*  
(Received 22 December 1992)

The first infrared vibrational photon echo experiments conducted in a liquid and a glass are reported. The experiments were performed on the CO stretching mode of tungsten hexacarbonyl at  $5.1 \mu\text{m}$  ( $1960 \text{ cm}^{-1}$ ) in 2-methyltetrahydrofuran over the temperature range 300 to 16 K using picosecond pulses from the free electron laser at Stanford University. In addition, the first vibrational population relaxation measurements spanning a temperature range that takes a system from a liquid to a supercooled liquid to a glass are reported.

PACS numbers: 42.50.Md, 33.70.Fd, 41.60.Cr, 64.70.Pf

Molecular vibrations are involved in a vast number of physical, chemical, and biological processes. Coupling between molecular vibrations and external mechanical degrees of freedom (heat bath) is responsible for the flow of energy into and out of molecules and for thermally activated processes. In spite of the importance of the coupling of molecular vibrations to a heat bath, relatively little is known about the dynamic aspects of molecular vibrations in condensed matter systems. What is known is mainly restricted to vibrational lifetime measurements in crystalline solids at low temperature [1].

Here we report the first infrared (ir) vibrational photon echo experiments conducted in a liquid and glass as well as temperature-dependent pump-probe experiments. The experiments examined the optical dephasing of the vibrational transition and the vibrational population relaxation of the CO asymmetric stretching mode of tungsten hexacarbonyl  $[\text{W}(\text{CO})_6]$  in 2-methyltetrahydrofuran (2-MTHF). The experiments were performed at a wavelength of  $5.1 \mu\text{m}$  ( $1960 \text{ cm}^{-1}$ ) at temperatures from 16 to 300 K using the superconducting-linear-accelerator-pumped free electron laser (FEL) at Stanford University.

In general, coupling of molecular vibrations to an external bath is substantially weaker than the coupling of electronic states. This is demonstrated by the fact that vibrational transition energies have a much smaller percentage of gas-to-"crystal" shifts than electronic transitions. The weaker coupling makes it possible to perform photon echoes on vibrational transitions of a molecule dissolved in a liquid using relatively long pulses (3 ps) that have narrow enough bandwidths so that only a well-defined pair of states is coherently coupled by the radiation field. Thus, the observed dephasing of the vibrational transition, with the contribution from population relaxation removed, arises from coupling to the heat bath. By passing through the glass-liquid transition, it is possible to observe how the change of state influences the vibrational dynamics.

The FEL used for these experiments [2,3] is a tunable

source of picosecond ir pulses. The FEL emits a 2 ms macropulse at 10 Hz. Each macropulse consists of  $\sim 0.5 \mu\text{J}$  micropulses at a repetition rate of 11.8 MHz. The micropulses were measured to be Gaussian 2.7 ps transform limited pulses. The micropulse repetition rate of 11.8 MHz was reduced to 50 kHz by an acousto-optic modulator single pulse selector. Thus, the effective experimental repetition rate was 1 kHz.

Both photon echo and pump-probe experiments require two input pulses, one of which is variably delayed. The single ir pulse was beam split. The reflected pulse (the probe pulse or second pulse in the echo sequence) was passed down a computer-controlled stepper-motor delay line. The transmitted pulse (the pump pulse or first pulse in the echo sequence) was chopped at half the single pulse rate by another AOM. The spot size was  $200 \mu\text{m}$ . For the pump-probe experiment, the pump pulse energy was 200 nJ and the probe energy was 20 nJ. The maximum change in transmitted intensity was less than 4%. For the photon echo experiment, the first pulse was 60 nJ and the second pulse was 150 nJ.

The signals were detected using an amplified liquid-nitrogen-cooled indium antimonide detector. In both experiments, the pulses were crossed at a small angle. For the pump-probe experiment, the detector was placed directly in the transmitted probe beam. For the photon echo, the detector was placed at the location determined by the wave vector matching condition  $\mathbf{k}_4 = 2\mathbf{k}_2 - \mathbf{k}_1$ , where  $\mathbf{k}_1$ ,  $\mathbf{k}_2$ , and  $\mathbf{k}_4$  are the wave vectors of the second pulse, the first pulse, and the photon echo pulse, respectively. The echo signal vanished when either beam was blocked. To check for power artifacts, the intensity of the excitation pulses was reduced by a factor of 2 and no change in the decay constants was observed for either the pump-probe or photon echo experiment. The echo intensity was reduced by a factor of 8 by the factor of 2 reduction in intensity, demonstrating that the echo experiments are in the low flip angle limit. The repetition rate of the pulses was also reduced by a factor of 2. No change in

signal for either type of experiment was observed.

Experiments were performed using  $4.0 \times 10^{-3}$  M  $W(CO)_6$  in 2-MTHF (Aldrich). This concentration gave an optical density of 0.8 at the absorption maximum for the sample thickness of 100  $\mu\text{m}$ . A thin sample was used to minimize the solvent background absorbance. Experiments were also performed at room temperature with more dilute concentrations of  $1.0 \times 10^{-3}$  and  $4.0 \times 10^{-4}$  M and no change in decay rate was observed. Experiments conducted on 2-MTHF with no  $W(CO)_6$  gave no signal in either type of experiment. All experiments were performed by rapidly cooling the sample in a variable temperature cryostat to the lowest temperature and then increasing the temperature. Therefore, the glass transition temperature was approached from below. The 2-MTHF was never observed to crystallize.

Figure 1 shows photon echo data taken at 16 K, and the inset shows a semilogarithmic plot of the data. The signal-to-noise ratio is very good, comparable to data taken on electronic transitions using conventional lasers. Data taken at other temperatures are equally good. The echo decay is a single exponential following a very fast feature around  $\tau=0$ . The photon echo signal decays as  $I(\tau) = I_0 \exp(-4\tau/T_2)$  where  $T_2$  is the homogeneous dephasing time [4]. In Fig. 1, the data decay in 15 ps yielding a  $T_2$  of 60 ps. The homogeneous linewidth ( $1/\pi T_2$ ) is 5.2 GHz. This is in contrast to the inhomogeneously broadened absorption line which is an  $18 \text{ cm}^{-1}$  Gaussian at 16 K, narrowing to  $15 \text{ cm}^{-1}$  at 300 K. The pure dephasing time  $T_2^*$  can be found by removing the contribution to  $T_2$  from the population decay of the excited vibrational state using the relation

$$1/\pi T_2 = 1/\pi T_2^* + 1/2\pi T_1, \quad (1)$$

where  $T_1$  is the excited vibrational state lifetime mea-

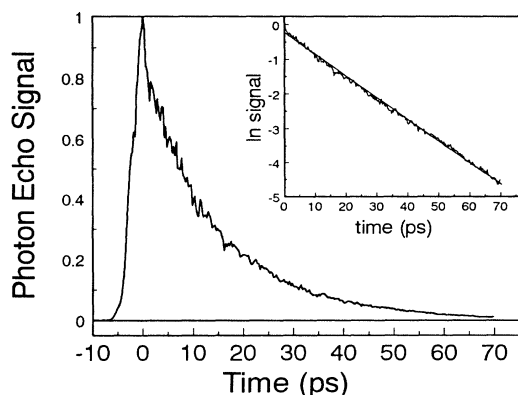


FIG. 1. Vibrational photon echo decay data taken of  $W(CO)_6$  in 2-MTHF at 16 K. The inset is a semilogarithmic plot showing the data decay exponentially. The signal decays with a 15 ps time constant, yielding a homogeneous dephasing time  $T_2=60$  ps and a homogeneous linewidth ( $1/\pi T_2$ ) of 5.2 GHz.

sured with the pump-probe experiments. At 16 K,  $T_1$  is 44 ps. Using Eq. (1), this gives a pure dephasing time  $T_2^*$  contribution to the homogeneous linewidth ( $1/\pi T_2^*$ ) of 1.6 GHz.

Figure 2 shows temperature-dependent echo data plotted as linewidths. The open squares are the homogeneous linewidths  $1/\pi T_2$ , and the filled squares are the pure dephasing linewidths  $1/\pi T_2^*$  calculated using Eq. (1) (see Fig. 3 below for  $T_1$  values). The vertical line at 88 K marks the glass-to-liquid transition temperature  $T_g$ . Although the time resolution was insufficient to determine the echo decay time above 140 K, it was possible to make photon echo decay measurements in the liquid state 50 K above  $T_g$ . The observation of the photon echo signal in the liquid demonstrates that vibrational lines in liquids can be inhomogeneously broadened.

As shown in Fig. 2, the linewidths increase gradually with temperature below  $T_g$ . Although there are limited data above  $T_g$ , the temperature dependence becomes much steeper. With the available data, it is not clear whether the behavior is discontinuous at  $T_g$ . Homogeneous dephasing of *electronic* transitions of chromophores in organic glasses at low temperatures (1 to 20 K) is described by the sum of a power law and an exponentially activated process. The expression used to fit electronic dephasing data is [5,6]

$$1/\pi T_2^* = aT^a + b \exp(-\Delta E/kt) / [1 - \exp(-\Delta E/kt)]. \quad (2)$$

For *electronic* transitions, the power law portion of Eq. (2) arises from the dynamics of the tunneling two-level systems (TLS) in the glass [7-10]. Typical values of  $a$  are 1.2 to 1.5 [5,11-13]. The exponentially activated process is due to coupling to low frequency phonons [5,6,14]. Typical values of  $\Delta E$  for *electronic* transitions fall in the range of 10 to 40  $\text{cm}^{-1}$  [5,11,14].

The solid line through the vibrational pure dephasing data was determined by fitting the data by Eq. (2). The

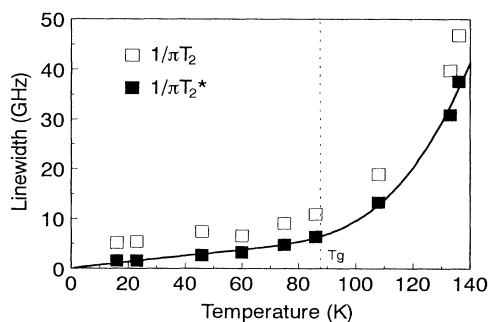


FIG. 2. Temperature-dependent photon echo data displayed as linewidths. The open squares are the total homogeneous linewidths. The filled squares are the pure dephasing linewidths with lifetime contribution removed. The line through the data is a fit by Eq. (2). The vertical line indicates the glass transition temperature of 88 K.

fit shown in Fig. 2 has  $\alpha=0.9$  and  $\Delta E = 540 \text{ cm}^{-1}$ . However, given the limited data above  $T_g$ , it is also possible to obtain a fit with a somewhat smaller  $\Delta E$  and  $\alpha \approx 1$ . The data display power law behavior almost to  $T_g$ . The power-law behavior of electronic dephasing at a temperature of a few degrees K is caused by TLS dynamics. As for low temperature heat capacity data,  $\alpha$  is approximately 1. The dephasing of the vibrational transition data displays power law behavior to much higher temperature with  $\alpha \approx 1$ . It is possible that the power law dephasing of the vibrational transition at these elevated temperatures is also caused by TLS dynamics. Here the power law is not masked by the activated processes at elevated temperatures since  $\Delta E$  is so large.

If Eq. (2) is the appropriate form to describe the data, then the resulting activation energy of  $540 \text{ cm}^{-1}$  is far too large to correspond to a phonon or pseudo local mode. The magnitude of  $\Delta E$  is in the range of molecular vibrations. Both  $\text{W}(\text{CO})_6$  and 2-MTHF have a variety of low frequency modes. By coincidence, both have a mode at  $\sim 580 \text{ cm}^{-1}$  [15,16]. Either of these modes could have energies within the error of the activation energy obtained from the fit. Both  $\text{W}(\text{CO})_6$  and 2-MTHF have a number of lower frequency modes as well as the  $580 \text{ cm}^{-1}$  modes. These modes will be thermally populated at lower temperatures. However, to cause dephasing, a mode of either  $\text{W}(\text{CO})_6$  or 2-MTHF must be quadratically coupled to the CO stretching mode being probed by the photon echo experiments; i.e., excitation of another mode of the system must cause a frequency shift of the CO stretching mode. Thus, the other modes may have such weak coupling to the CO stretching mode that they do not cause pure dephasing.

Figure 3 shows the temperature dependence of the pump-probe data from 16 to 300 K. Below 140 K, the decays are rigorously single exponential and were used as the  $T_1$  values for the pure dephasing linewidth calcula-

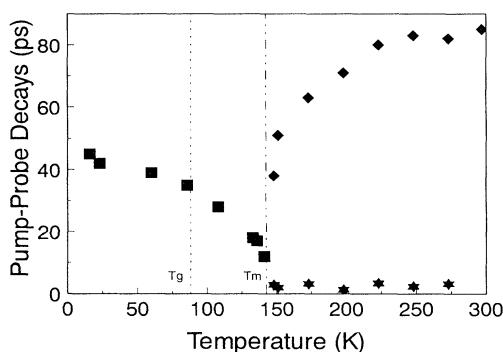


FIG. 3. Temperature-dependent pump-probe vibrational lifetime data. Below  $\sim 140$  K, the decays are single exponentials and are shown as squares. Above  $\sim 140$  K all decays are biexponential and both decay times are shown. The stars show the fast component, and the diamonds show the slower component. The two decay components have equal amplitudes.

tions displayed in Fig. 2. However, above 140 K the data are biexponential decays with the two components having approximately equal amplitudes. Above 140 K, both components of the biexponentials are plotted in Fig. 3. The decay of the pump-probe signal shows a clear discontinuity at  $\sim 140$  K.

If vibrational relaxation directly repopulates the ground state, the decay will be a single exponential. However, if there is an intermediate level in the relaxation pathway, the decay can be biexponential if population of the intermediate causes a shift in the CO stretching frequency. One component is the rate of leaving the excited state into a longer living intermediate state, which turns off the stimulated emission, and the other component is the ground state population recovery. These two components should have equal amplitudes, which is consistent with the data. (If all intermediate states have very short lifetimes, the decay will also appear to be single exponential.)

Because of the limits imposed by the pulse duration, the fast component of the biexponential decay cannot be determined precisely. What is clear is that the slow component speeds up dramatically as the temperature is lowered, and the fast component seems to slow down. The remarkable fact is that the discontinuity in the data takes place at what would be the melting point of crystalline 2-MTHF,  $\sim 140$  K [17]. However, 2-MTHF does not crystallize, but rather supercools and then forms a glass at 88 K [18]. The properties of liquids should be continuous in going from the liquid to the supercooled liquid. Clearly, the vibrational decay is not continuous.

If the fast decay component slows down and the slow component becomes extremely fast below  $\sim 140$  K, the data will take on the appearance of a single exponential, as observed. Generally, one might expect a vibrational decay to become slower as the temperature is decreased because of reduced phonon occupation numbers. Vibrational relaxation requires coupling between internal  $\text{W}(\text{CO})_6$  modes and the bath modes. It is necessary to convert the vibrational energy into heat. Since the vibrational energy is large, it is unlikely that the vibrational relaxation involves the direct, simultaneous excitation of many bath phonons. A more likely process involves the excitation of at least one vibrational mode of the 2-MTHF and one or more phonons. This requires coupling between the  $\text{W}(\text{CO})_6$  vibrations and the 2-MTHF vibrations. As the temperature is decreased from room temperature, the viscosity of the liquid increases, and the 2-MTHF rotational diffusion rate slows dramatically. If the matrix element that couples the CO stretching mode to a 2-MTHF vibration is strongly dependent on orientation, then rapid rotation of the 2-MTHF at high temperatures could result in an orientationally averaged matrix element that is small. When the viscosity becomes large, favorable orientations will exist for long enough to enhance the coupling and therefore increase the rate of vibrational relaxation. This will be particularly impor-

tant if the intermolecular interactions between  $W(CO)_6$  and 2-MTHF favor local liquid structures having relative orientations that yield large intermolecular vibrational coupling matrix elements.

In conclusion, vibrational photon echoes, as presented here, are a new method for examining molecular vibrational dynamics in the liquid and glassy states of matter. These initial experiments will be extended to broader ranges of temperature and time and to other solvents and solutes. Experiments will also be conducted on the vibrations of pure liquids and glasses. In addition to photon echoes, stimulated echoes will be employed to examine spectral diffusion, and comparisons of vibrational photon echoes with ir hole burning experiments will aid in elucidating the underlying dynamics that give rise to hole widths. The use of condensed matter vibrational optical coherence experiments will enhance our understanding of molecular vibrations in the same manner as magnetic resonance coherence experiments and optical coherence experiments have broadened our knowledge of spin systems and electronic excitations.

This work was funded by the Medical Free Electron Laser program through the Office of Naval Research (Grant No. N00014-91-C-0170). David Zimdars, A. Tokmakoff, S. Chen, S. R. Greenfield, and M. D. Fayer would like to acknowledge additional support from the National Science Foundation, Division of Material Research (Grant No. DMR90-22675) and the Office of Naval Research, Physics Division (Grant No. N00014-89-J1119).

---

[1] D. D. Dlott, *Laser Spectroscopy of Solids II*, edited by W. Yen, Topics in Applied Physics Vol. 65 (Springer, Berlin, 1989), p. 167.

- [2] R. L. Swent, H. A. Schwettman, and T. I. Smith, in *Short-Wavelength Radiation Sources*, edited by P. Sprangle, SPIE Proceedings Vol. 1552 (SPIE, Bellingham, WA, 1991), p. 24.
- [3] D. D. Dlott and M. D. Fayer, *IEEE J. Quantum Electron.* **27**, 2697 (1991).
- [4] I. Abella, N. A. Kurnit, and S. R. Hartmann, *Phys. Rev.* **141**, 391 (1966).
- [5] L. R. Narasimhan, K. A. Littau, D. W. Pack, Y. S. Bai, A. Elschner, and M. D. Fayer, *Chem. Rev.* **90**, 439 (1990).
- [6] B. Jackson and R. Silbey, *Chem. Phys. Lett.* **99**, 331 (1983).
- [7] M. Berg, C. A. Walsh, L. R. Narasimhan, K. A. Littau, and M. D. Fayer, *J. Chem. Phys.* **88**, 1564 (1987).
- [8] R. Jankowiak, L. Shu, M. J. Kenney, and G. J. Small, *J. Lumin.* **36**, 293 (1987).
- [9] D. L. Huber, M. M. Broer, and B. Golding, *Phys. Rev. Lett.* **52**, 2281 (1984).
- [10] D. W. Pack, L. R. Narasimhan, and M. D. Fayer, *J. Chem. Phys.* **92**, 4125 (1990).
- [11] S. R. Greenfield, Y. S. Bai, and M. D. Fayer, *Chem. Phys. Lett.* **170**, 133 (1990).
- [12] H. P. H. Thijssen, R. van den Berg, and S. Völker, *Chem. Phys. Lett.* **103**, 23 (1983).
- [13] W. S. Brocklesby, B. Golding, and J. R. Simpson, *J. Lumin.* **45**, 54 (1990).
- [14] W. H. Hesselink and D. A. Wiersma, *J. Chem. Phys.* **73**, 648 (1980).
- [15] P. S. Braterman, *Metal Carbonyl Spectra* (Academic, New York, 1975), p. 182.
- [16] *Handbook of Data on Organic Compounds*, edited by R. C. Weast and J. C. Grasselli (CRC Press, Boca Raton, FL, 1985), 2nd ed., p. 2770.
- [17] E. V. Whitehead, R. A. Dern, and F. A. Fidler, *J. Am. Chem. Soc.* **73**, 3632 (1951).
- [18] A. C. Ling and J. E. Willard, *J. Phys. Chem.* **72**, 1918 (1968).